

# Observational constraints on Hořava-Lifshitz cosmology

Sourish Dutta<sup>1,\*</sup> and Emmanuel N. Saridakis<sup>2,†</sup>

<sup>1</sup>*Department of Physics and Astronomy, Vanderbilt University, Nashville, TN 37235*

<sup>2</sup>*Department of Physics, University of Athens, GR-15771 Athens, Greece*

(Dated: November 2, 2018)

We use observational data from Type Ia Supernovae (SNIa), Baryon Acoustic Oscillations (BAO), and Cosmic Microwave Background (CMB), along with requirements of Big Bang Nucleosynthesis (BBN), to constrain the cosmological scenarios governed by Hořava-Lifshitz gravity. We consider both the detailed and non-detailed balance versions of the gravitational sector, and we include the matter and radiation sectors. We conclude that the detailed-balance scenario cannot be ruled out from the observational point of view, however the corresponding likelihood contours impose tight constraints on the involved parameters. The scenario beyond detailed balance is compatible with observational data, and we present the corresponding stringent constraints and contour-plots of the parameters. Although this analysis indicates that Hořava-Lifshitz cosmology can be compatible with observations, it does not enlighten the discussion about its possible conceptual and theoretical problems.

PACS numbers: 98.80.-k, 04.60.Bc, 04.50.Kd

## I. INTRODUCTION

Recently, a power-counting renormalizable, ultra-violet (UV) complete theory of gravity was proposed by Hořava in [1, 2, 3, 4]. Although presenting an infrared (IR) fixed point, namely General Relativity, in the UV the theory possesses a fixed point with an anisotropic, Lifshitz scaling between time and space. Due to these novel features, there has been a large amount of effort in examining and extending the properties of the theory itself [5, 6, 7, 8, 9, 10, 11, 12, 13, 14, 15, 16, 17, 18, 19, 20, 21, 22, 23, 24, 25, 26, 27, 28]. Additionally, application of Hořava-Lifshitz gravity as a cosmological framework gives rise to Hořava-Lifshitz cosmology, which proves to lead to interesting behavior [29, 30]. In particular, one can examine specific solution subclasses [31, 32, 33, 34, 35, 36, 37, 38, 39, 40], the phase-space behavior [41, 42], the gravitational wave production [43, 44, 45, 46, 47, 48], the perturbation spectrum [49, 50, 51, 52, 53, 54, 55, 56, 57], the matter bounce [58, 59, 60, 61], the black hole properties [62, 63, 64, 65, 66, 67, 68, 69, 70, 71, 72, 73], the dark energy phenomenology [74, 75, 76, 77], the astrophysical phenomenology [78, 79, 80, 81], the thermodynamic properties [82, 83, 84] etc. However, despite this extended research, there are still many ambiguities if Hořava-Lifshitz gravity is reliable and capable of a successful description of the gravitational background of our world, as well as of the cosmological behavior of the universe [11, 13, 15, 24, 85, 86].

Although the discussion about the foundations and the possible conceptual and phenomenological problems of Hořava-Lifshitz gravity and cosmology is still open in

the literature, it is worth investigating in a systematic way the constraints imposed by observations in a universe governed by Hořava gravity. Thus, in the present work we use Big Bang Nucleosynthesis conditions, together with Type Ia Supernovae (SNIa), Baryon Acoustic Oscillations (BAO) and Cosmic Microwave Background (CMB) data, in order to construct the corresponding probability contour-plots for the parameters of the theory. Furthermore, in order to be general and model-independent, we perform our analysis with and without the detailed-balance condition. As we will show, both the detailed-balance and beyond-detailed-balance formulations are compatible with observations, however under tight constraints on the model parameters.

The paper is organized as follows: In section II we present the basic ingredients of Hořava-Lifshitz cosmology, extracting the Friedmann equations, and describing the dark matter and dark energy dynamics. In section III we constrain both the detailed-balance and the beyond-detailed-balance formulations from the observational point of view. Finally, section IV is devoted to the summary of the obtained results.

## II. HOŘAVA-LIFSHITZ COSMOLOGY

Let us present the scenario where the cosmological evolution is governed by Hořava-Lifshitz gravity [29, 30]. The dynamical variables are the lapse and shift functions,  $N$  and  $N_i$  respectively, and the spatial metric  $g_{ij}$  (roman letters indicate spatial indices). In terms of these fields the full metric is written as:

$$ds^2 = -N^2 dt^2 + g_{ij}(dx^i + N^i dt)(dx^j + N^j dt), \quad (1)$$

where indices are raised and lowered using  $g_{ij}$ . The scaling transformation of the coordinates reads:

$$t \rightarrow l^3 t \quad \text{and} \quad x^i \rightarrow l x^i. \quad (2)$$

\*Electronic address: sourish.d@gmail.com

†Electronic address: msaridak@phys.uoa.gr

### A. Detailed Balance

The gravitational action is decomposed into a kinetic and a potential part as  $S_g = \int dt d^3x \sqrt{g} N (\mathcal{L}_K + \mathcal{L}_V)$ . The assumption of detailed balance [3] reduces the possible terms in the Lagrangian, and it allows for a quantum inheritance principle [1], since the  $(D+1)$ -dimensional theory acquires the renormalization properties of the  $D$ -dimensional one. Under the detailed balance condition the full action of Hořava-Lifshitz gravity is given by

$$S_g = \int dt d^3x \sqrt{g} N \left\{ \frac{2}{\kappa^2} (K_{ij} K^{ij} - \lambda K^2) + \frac{\kappa^2}{2w^4} C_{ij} C^{ij} - \frac{\kappa^2 \mu}{2w^2} \frac{\epsilon^{ijk}}{\sqrt{g}} R_{il} \nabla_j R_k^l + \frac{\kappa^2 \mu^2}{8} R_{ij} R^{ij} + \frac{\kappa^2 \mu^2}{8(1-3\lambda)} \left[ \frac{1-4\lambda}{4} R^2 + \Lambda R - 3\Lambda^2 \right] \right\}, \quad (3)$$

where

$$K_{ij} = \frac{1}{2N} (g_{ij} - \nabla_i N_j - \nabla_j N_i) \quad (4)$$

is the extrinsic curvature and

$$C^{ij} = \frac{\epsilon^{ijk}}{\sqrt{g}} \nabla_k (R_i^j - \frac{1}{4} R \delta_i^j) \quad (5)$$

the Cotton tensor, and the covariant derivatives are defined with respect to the spatial metric  $g_{ij}$ .  $\epsilon^{ijk}$  is the totally antisymmetric unit tensor,  $\lambda$  is a dimensionless constant and the variables  $\kappa$ ,  $w$  and  $\mu$  are constants with mass dimensions  $-1$ ,  $0$  and  $1$ , respectively. Finally, we mention that in action (3) we have performed the usual analytic continuation of the parameters  $\mu$  and  $w$  of the original version of Hořava-Lifshitz gravity, since such a procedure is required in order to obtain a realistic cosmology [31, 35, 68, 82] (although it could fatally affect the gravitational theory itself). Therefore, in the present work  $\Lambda$  is a positive constant, which as usual is related to the cosmological constant in the IR limit.

In order to add the matter component (including both dark and baryonic matter) in the theory one can follow two equivalent approaches. The first is to introduce a scalar field [29, 30] and thus attribute to dark matter a dynamical behavior, with its energy density  $\rho_m$  and pressure  $p_m$  defined through the field kinetic and potential energy. Although such an approach is theoretically robust, it is not suitable from the phenomenological point of view since it requires special matter-potentials in order to acquire an almost constant matter equation-of-state parameter ( $w_m = p_m/\rho_m$ ) as it is suggested by observations. In the second approach one adds a cosmological stress-energy tensor to the gravitational field equations, by demanding to recover the usual general relativity formulation in the low-energy limit [13, 41]. Thus, this matter-tensor is a hydrodynamical approximation with  $\rho_m$  and  $p_m$  (or  $\rho_m$  and  $w_m$ ) as parameters. Similarly, one can additionally include the standard-model-radiation component (corresponding to photons and neutrinos), with the additional parameters  $\rho_r$  and  $p_r$  (or  $\rho_r$

and  $w_r$ ). Such an approach, although not fundamental, is better for a phenomenological analysis, such the one performed in this work.

Now, in order to focus on cosmological frameworks, we impose the so called projectability condition [11] and use an FRW metric,

$$N = 1, \quad g_{ij} = a^2(t) \gamma_{ij}, \quad N^i = 0, \quad (6)$$

with

$$\gamma_{ij} dx^i dx^j = \frac{dr^2}{1-Kr^2} + r^2 d\Omega_2^2, \quad (7)$$

where  $K <, =, > 0$  corresponding to open, flat, and closed universe respectively (we have adopted the convention of taking the scale factor  $a(t)$  to be dimensionless and the curvature constant  $K$  to have mass dimension 2). By varying  $N$  and  $g_{ij}$ , we obtain the equations of motion:

$$H^2 = \frac{\kappa^2}{6(3\lambda-1)} (\rho_m + \rho_r) + \frac{\kappa^2}{6(3\lambda-1)} \left[ \frac{3\kappa^2 \mu^2 K^2}{8(3\lambda-1)a^4} + \frac{3\kappa^2 \mu^2 \Lambda^2}{8(3\lambda-1)} \right] - \frac{\kappa^4 \mu^2 \Lambda K}{8(3\lambda-1)^2 a^2}, \quad (8)$$

$$\dot{H} + \frac{3}{2} H^2 = -\frac{\kappa^2}{4(3\lambda-1)} (w_m \rho_m + w_r \rho_r) - \frac{\kappa^2}{4(3\lambda-1)} \left[ \frac{\kappa^2 \mu^2 K^2}{8(3\lambda-1)a^4} - \frac{3\kappa^2 \mu^2 \Lambda^2}{8(3\lambda-1)} \right] - \frac{\kappa^4 \mu^2 \Lambda K}{16(3\lambda-1)^2 a^2}, \quad (9)$$

where we have defined the Hubble parameter as  $H \equiv \frac{\dot{a}}{a}$ . As usual,  $\rho_m$  (dark plus baryonic matter) follows the standard evolution equation

$$\dot{\rho}_m + 3H(\rho_m + p_m) = 0, \quad (10)$$

while  $\rho_r$  (standard-model radiation) follows

$$\dot{\rho}_r + 3H(\rho_r + p_r) = 0. \quad (11)$$

Finally, concerning the dark-energy sector we can define

$$\rho_{DE} \equiv \frac{3\kappa^2 \mu^2 K^2}{8(3\lambda-1)a^4} + \frac{3\kappa^2 \mu^2 \Lambda^2}{8(3\lambda-1)} \quad (12)$$

$$p_{DE} \equiv \frac{\kappa^2 \mu^2 K^2}{8(3\lambda-1)a^4} - \frac{3\kappa^2 \mu^2 \Lambda^2}{8(3\lambda-1)}. \quad (13)$$

The term proportional to  $a^{-4}$  is the usual ‘‘dark radiation term’’, present in Hořava-Lifshitz cosmology [29, 30], while the constant term is just the explicit cosmological constant. Therefore, in expressions (12),(13) we have

defined the energy density and pressure for the effective dark energy, which incorporates the aforementioned contributions. Finally, note that using (12),(13) it is straightforward to see that these dark energy quantities satisfy the standard evolution equation:

$$\dot{\rho}_{DE} + 3H(\rho_{DE} + p_{DE}) = 0. \quad (14)$$

Using the above definitions, we can re-write the Friedmann equations (8),(9) in the standard form:

$$H^2 = \frac{\kappa^2}{6(3\lambda - 1)} [\rho_m + \rho_r + \rho_{DE}] - \frac{\kappa^4 \mu^2 \Lambda K}{8(3\lambda - 1)^2 a^2} \quad (15)$$

$$\dot{H} + \frac{3}{2}H^2 = -\frac{\kappa^2}{4(3\lambda - 1)} [p_m + p_r + p_{DE}] - \frac{\kappa^4 \mu^2 \Lambda K}{16(3\lambda - 1)^2 a^2}. \quad (16)$$

Therefore, if we require these expressions to coincide with the standard Friedmann equations, in units where  $c = 1$  we set [29, 30]:

$$G = \frac{\kappa^2}{16\pi(3\lambda - 1)} \quad (17)$$

$$\mu^2 \Lambda = \frac{1}{32\pi^2 G^2},$$

with  $G$  the usual Newton's constant. Note that the running of the light speed with  $\lambda$ , is not a problem, since in this work we will remain in the phenomenologically relevant case of  $\lambda = 1$ .

## B. Beyond Detailed Balance

The aforementioned formulation of Hořava-Lifshitz cosmology has been performed under the imposition of the detailed-balance condition. However, in the literature there is a discussion whether this condition leads to reliable results or if it is able to reveal the full information of Hořava-Lifshitz gravity [29, 30]. Therefore, one needs to investigate also the Friedmann equations in the case where detailed balance is relaxed. In such a case one can in general write [11, 13, 15, 41, 42]:

$$H^2 = \frac{2\sigma_0}{(3\lambda - 1)} (\rho_m + \rho_r) + \frac{2}{(3\lambda - 1)} \left[ \frac{\sigma_1}{6} + \frac{\sigma_3 K^2}{6a^4} + \frac{\sigma_4 K}{6a^6} \right] + \frac{\sigma_2}{3(3\lambda - 1)} \frac{K}{a^2} \quad (18)$$

$$\dot{H} + \frac{3}{2}H^2 = -\frac{3\sigma_0}{(3\lambda - 1)} (w_m \rho_m + w_r \rho_r) - \frac{3}{(3\lambda - 1)} \left[ -\frac{\sigma_1}{6} + \frac{\sigma_3 K^2}{18a^4} + \frac{\sigma_4 K}{6a^6} \right] + \frac{\sigma_2}{6(3\lambda - 1)} \frac{K}{a^2}, \quad (19)$$

where  $\sigma_0 \equiv \kappa^2/12$ , and the constants  $\sigma_i$  are arbitrary (with  $\sigma_2$  being negative). Note that one could absorb the factor of 6 in redefined parameters, but we prefer to keep it in order to coincide with the notation of [13, 41]. As we observe, the effect of the detailed-balance relaxation is the decoupling of the coefficients, together with the appearance of a term proportional to  $a^{-6}$ . In this case the corresponding quantities for dark energy are generalized to

$$\rho_{DE}|_{\text{non-db}} \equiv \frac{\sigma_1}{6} + \frac{\sigma_3 K^2}{6a^4} + \frac{\sigma_4 K}{6a^6} \quad (20)$$

$$p_{DE}|_{\text{non-db}} \equiv -\frac{\sigma_1}{6} + \frac{\sigma_3 K^2}{18a^4} + \frac{\sigma_4 K}{6a^6}. \quad (21)$$

Therefore, it is easy to see that

$$\dot{\rho}_{DE}|_{\text{non-db}} + 3H(\rho_{DE}|_{\text{non-db}} + p_{DE}|_{\text{non-db}}) = 0. \quad (22)$$

Finally, if we force (18),(19) to coincide with the standard Friedmann equations, we result to:

$$G = \frac{6\sigma_0}{8\pi(3\lambda - 1)} \quad (23)$$

$$\sigma_2 = -3(3\lambda - 1).$$

## III. OBSERVATIONAL CONSTRAINTS

Having presented the cosmological equations of a universe governed by Hořava-Lifshitz gravity, both with and without the detailed-balance condition, we now proceed to study the observational constraints on the model parameters. This is performed in the following two subsections, for the detailed and non-detailed balance scenarios separately. We mention that since the cosmological observations lie deep inside the IR, in the following we set the running parameter  $\lambda$  to 1.

### A. Constraints on Detailed-Balance scenario

We work in the usual units suitable for observational comparisons, namely setting  $8\pi G = 1$  (we have already set  $c = 1$  in order to obtain (17)). This allows us to reduce the parameter space, since in this case (17) lead to:

$$\kappa^2 = 4 \quad (24)$$

$$\mu^2 \Lambda = 2.$$

Inserting these relations into Friedmann equation (8) we obtain

$$H^2 = \frac{1}{3} (\rho_m + \rho_r) + \frac{1}{3} \left( \frac{3K^2}{2\Lambda a^4} + \frac{3\Lambda}{2} \right) - \frac{K}{a^2}. \quad (25)$$

In terms of the usual density parameters ( $\Omega_m \equiv \rho_m/(3H^2)$ ,  $\Omega_K \equiv -K/(H^2 a^2)$ ,  $\Omega_r \equiv \rho_r/(3H^2)$ ) this expression becomes:

$$1 - \Omega_m - \Omega_r - \Omega_K = \frac{1}{H^2} \left( \frac{K^2}{2\Lambda a^4} + \frac{\Lambda}{2} \right). \quad (26)$$

Finally, applying this relation at present time and setting the current scale factor  $a_0 = 1$  we get:

$$1 - \Omega_{m0} - \Omega_{r0} - \Omega_{K0} = \frac{1}{H_0^2} \left( \frac{K^2}{2\Lambda} + \frac{\Lambda}{2} \right), \quad (27)$$

where a 0-subscript denotes the present value of the corresponding quantity.

As was mentioned above, we have used the analytic continuation, as a result of which  $\Lambda$  is positive. Thus, relation (27) can in principle be satisfied by a suitable choice of  $\Lambda$ . However, note that without the analytic continuation (and therefore with a negative  $\Lambda$ ) relation (27) could never be satisfied (as expected, since in this case the theory would not have the  $\lambda = 1$  IR, general-relativity limit), and this offers another indication, from the phenomenological point of view, for the necessity of the analytic continuation in the detailed-balance version of Hořava-Lifshitz cosmology.

In order to proceed to the elaboration of observational data, we consider as usual the matter (dark plus baryonic) component to be dust, that is  $w_m \approx 0$ , and similarly for the standard-model radiation we consider  $w_r = 1/3$ , where both assumptions are valid in the epochs in which observations focus. Therefore, the corresponding evolution equations (10),(11) give  $\rho_m = \rho_{m0}/a^3$  and  $\rho_r = \rho_{r0}/a^4$  respectively. Finally, instead of the scale factor it proves convenient to use the redshift  $z$  as the independent variable, which is given by  $1+z \equiv a_0/a = 1/a$ . Inserting these into Friedmann equation (25) we obtain

$$H^2 = H_0^2 \left\{ \Omega_{m0}(1+z)^3 + \Omega_{r0}(1+z)^4 + \Omega_{K0}(1+z)^2 + \left[ \omega + \frac{\Omega_{K0}^2}{4\omega}(1+z)^4 \right] \right\}, \quad (28)$$

where we have also introduced the dimensionless parameter  $\omega \equiv \Lambda/(2H_0^2)$ . Thus, the constraint (27) can be rewritten as:

$$\Omega_{m0} + \Omega_{r0} + \Omega_{K0} + \omega + \frac{\Omega_{K0}^2}{4\omega} = 1. \quad (29)$$

As we have already mentioned above, the term  $\Omega_{K0}^2/(4\omega)$  is the coefficient of the dark radiation term, which is a characteristic feature of the Hořava-Lifshitz gravitational background. Since this dark radiation component has been present also during the time of nucleosynthesis, it is subject to bounds from Big Bang Nucleosynthesis (BBN). As discussed in more details in the Appendix, if the upper limit on the total amount of dark radiation allowed during BBN is expressed through the parameter  $\Delta N_\nu$  of the effective neutrino species [105, 106, 107, 108], then we obtain the following constraint :

$$\frac{\Omega_{K0}^2}{4\omega} = 0.135 \Delta N_\nu \Omega_{r0}. \quad (30)$$

Finally, we mention that as usual, the density parameter for standard model radiation (photons and three species

of neutrinos)  $\Omega_{r0}$  is entirely determined by  $\Omega_{m0}$ ,  $H_0$  and the measured value of the CMB temperature [87].

In most studies of dark energy models it is customary to ignore curvature (e.g.[88, 89, 90, 91, 92, 93, 94, 95]), especially concerning observational constraints. This practice is well motivated for at least two reasons. Firstly, most inflationary scenarios predict a high degree of spatial flatness. Secondly, the CMB data impose stringent constraints on spatial flatness in the context of constant- $w$  models (for example a combination of WMAP+BAO+SNIa data [87] provides the tight simultaneous constraints  $-0.0179 \leq \Omega_{K0} \leq 0.0081$  and  $-0.12 \leq 1+w \leq 0.14$ , both at 95% confidence).

However, it is important to keep in mind that owing to degeneracies in the CMB power spectrum (see [96] and references therein), the limits on curvature depend on assumptions regarding the underlying dark energy scenario. For example, if instead of a constant  $w$  one works with a linearly varying  $w$ , parameterized as  $w(a) = w_0 + (1-a)w_a$ , the error on  $\Omega_{K0}$  is much larger, on the order of a few percent [97, 98, 99]. The constraints on curvature for different parameterizations was studied in [100, 101, 102]. The authors of [102] showed that for some models of dark energy the constraint on the curvature is at the level of 5% around a flat universe, whereas for others the data are consistent with an open universe with  $\Omega_{K0} \sim 0.2$ . According to [98], geometrical tests such as the combination of the Hubble parameter  $H(z)$  and the angular diameter distance  $D_A(z)$ , using (future) data up to sufficiently high redshifts  $z \sim 2$ , might be able to disentangle curvature from dark energy evolution, though not in a model-independent way. [103, 104] highlight the pitfalls arising from ignoring curvature in studies of dynamical dark energy, and recommend treating  $\Omega_{K0}$  as a free parameter to be fitted along with the other model parameters.

In the present work, the spatial curvature plays a very crucial role, since, as it has been extensively stated in the literature [29, 30], Hořava-Lifshitz cosmology coincides completely with  $\Lambda$ CDM if one ignores curvature. Therefore, and following the discussion above, we choose to treat  $\Omega_{K0}$  as a free parameter.

In summary, the scenario at hand involves four parameters (we fix  $H_0$  by its 5-year WMAP best-fit values, given in Table 1 of [87]), namely  $\Omega_{m0}$ ,  $\Omega_{K0}$ ,  $\omega$  and  $\Delta N_\nu$ , subject to constraint equations (29) and (30). Therefore, only two of these parameters are independent. Although one would usually expect to be able to choose two of them at will, the non-linear nature of the constraint equations does not facilitate this, and one has no choice but to use  $\Omega_{m0}$  and  $\Delta N_\nu$  as free parameters. Inverting (29) and (30) to express  $\omega$  and  $\Omega_{K0}$  in terms of these independent parameters for a given curvature, we obtain:

$$\omega(K; \Omega_{m0}, \Delta N_\nu) = 1 - \Omega_{m0} - (1 - \Delta N_\nu)\Omega_{r0} - 0.73 \operatorname{sgn}(K) \sqrt{\Delta N_\nu} \sqrt{\Omega_{r0} - \Omega_{m0}\Omega_{r0} - \Omega_{r0}^2} \quad (31)$$

and

$$|\Omega_{K0}(\Omega_{m0}, \Delta N_\nu)| = \sqrt{0.54 \Delta N_\nu \Omega_{r0} \omega(\Omega_{m0}, \Delta N_\nu)}. \quad (32)$$

The BBN upper limit on  $\Delta N_\nu$  is  $-1.7 \leq \Delta N_\nu \leq 2.0$  [105, 106, 107, 108]. A negative value of  $\Delta N_\nu$  (which is usually associated with models involving decay of a massive particle) is not possible in the present model, since  $\omega$  (i.e.  $\Lambda$ ) is always positive. Additionally,  $\Delta N_\nu = 0$  corresponds to the zero curvature scenario (a non-interesting case since Hořava-Lifshitz cosmology with zero curvature becomes indistinguishable from  $\Lambda$ CDM).

In Fig. 1 and Fig 2 we use a combination of observational data from SNIa, BAO and CMB to construct likelihood contours for the parameters  $\Omega_{m0}$  and  $\Delta N_\nu$  for positive and negative curvatures respectively. These fig-

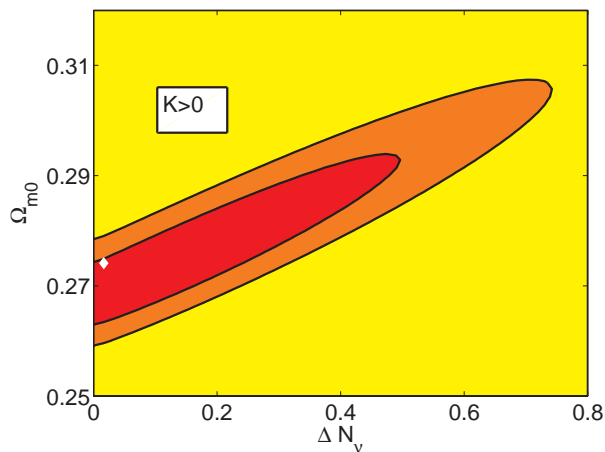


FIG. 1: (Color Online) *Contour plots of  $\Omega_{m0}$  vs  $\Delta N_\nu$  for positive curvature ( $K > 0$ ), under SNIa, BAO and CMB observational data. The yellow (light) region is excluded at the  $2\sigma$  level, and the orange (darker) region is excluded at the  $1\sigma$  level. The red (darkest) region is not excluded at either confidence level. The white diamond marks the best-fit point. The model parameters  $\omega \equiv \Lambda/(2H_0^2)$  and  $\Omega_{K0} \equiv -K/(H_0^2)$  are related to  $\Omega_{m0}$  and  $\Delta N_\nu$  through (31) and (32).*

ures show that the Hořava-Lifshitz cosmological scenario under the detailed balance condition is not ruled out by observations. However, they lead to tight constraints on the amount of dark radiation allowed at the time of nucleosynthesis (tighter than the corresponding limits from BBN), and thus to the parameter  $\Lambda$ . For example, the  $1\sigma$  limits on  $\Omega_{K0}$ ,  $\Lambda$  and  $\mu$  (which is actually connected to  $\Lambda$  through (17)) are presented in Table I. For convenience we have kept the factors of  $H_0$  and  $8\pi G$ . Thus, one can either use the usual ansatz  $8\pi G = H_0 = 1$ , or insert physical units using  $H_0 = 1.503 \times 10^{-42}$  GeV and  $8\pi G = 1.681 \times 10^{-37}$  GeV $^{-2}$ . In the later case, one obtains  $0 < \Lambda \lesssim 1.86 \times 10^{-9}$  eV $^4$  and  $3.30 \times 10^{60} \lesssim \mu < \infty$  for the positive curvature case, and similarly for the negative curvature one.

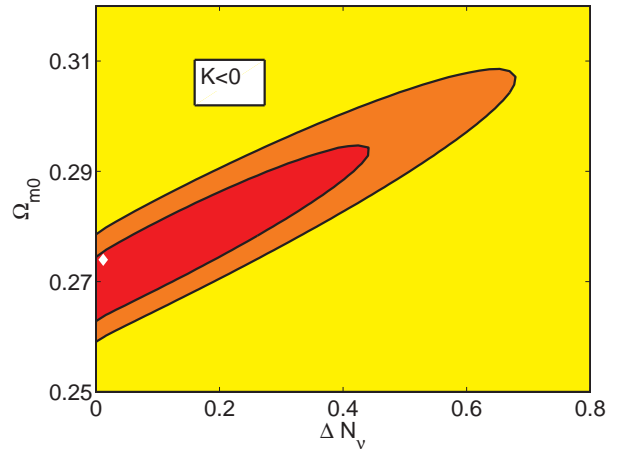


FIG. 2: (Color Online) *Contour plots of  $\Omega_{m0}$  vs  $\Delta N_\nu$  for negative curvature ( $K < 0$ ), under SNIa, BAO and CMB observational data. The yellow (light) region is excluded at the  $2\sigma$  level, and the orange (darker) region is excluded at the  $1\sigma$  level. The red region is not excluded at either confidence level. The white diamond marks the best-fit point. The model parameters  $\omega \equiv \Lambda/(2H_0^2)$  and  $\Omega_{K0} \equiv -K/(H_0^2)$  are related to  $\Omega_{m0}$  and  $\Delta N_\nu$  through (31) and (32).*

In conclusion, we have shown that Hořava-Lifshitz cosmology under the assumption of detailed-balance condition cannot fulfill observational requirements without the analytic continuation transformation. Under analytic continuation the observational constraints on the parameters are quite tight. This feature was already mentioned in [15], following qualitative theoretical arguments concerning the effective light speed in Hořava-Lifshitz framework, where it was stated that a fine tuning would be needed as a way out. The analysis of this section offers new, phenomenological indications towards the direction of tight constraints.

## B. Constraints on Beyond-Detailed-Balance scenario

In units where  $8\pi G = 1$  relations (23) give

$$\begin{aligned} \sigma_0 &= 1/3 \\ \sigma_2 &= -6. \end{aligned} \quad (33)$$

Using these values and following the procedure of the previous subsection, the Friedmann equation (18) can be written as

$$H^2 = H_0^2 \left\{ \Omega_{m0} (1+z)^3 + \Omega_{r0} (1+z)^4 + \Omega_{K0} (1+z)^2 + \left[ \omega_1 + \omega_3 (1+z)^4 + \omega_4 (1+z)^6 \right] \right\}. \quad (34)$$

In this expression we have introduced the dimensionless parameters  $\omega_1$ ,  $\omega_3$  and  $\omega_4$ , related to the model param-

$\kappa^2/(8\pi G)$	$\Omega_{K0}$	$(8\pi G/H_0^2) \Lambda$	$(H_0\sqrt{8\pi G}) \mu$
4	(0, 0.0038)	(0, 1.4189)	(1.1872, $\infty$ )
4	(-0.0039, 0)	(0, 1.4063)	(1.1925, $\infty$ )

TABLE I:  $1\sigma$  limits on the parameter values for the detailed-balance scenario, for positive and negative curvature.

ters  $\sigma_1$ ,  $\sigma_3$  and  $\sigma_4$  through:

$$\begin{aligned}\omega_1 &= \frac{\sigma_1}{6H_0^2} \\ \omega_3 &= \frac{\sigma_3 H_0^2 \Omega_{K0}^2}{6} \\ \omega_4 &= -\frac{\sigma_4 \Omega_{K0}}{6}.\end{aligned}\quad (35)$$

Furthermore, we consider the combination  $\omega_4$  to be positive, in order to ensure that the Hubble parameter is real for all redshifts.  $\omega_4 > 0$  is required also for the stability of the gravitational perturbations of the theory [13, 15]. For convenience we moreover assume  $\sigma_3 \geq 0$ , that is  $\omega_3 \geq 0$ .

The scenario at hand involves the following parameters:  $H_0$ ,  $\Omega_{m0}$ ,  $\Omega_{K0}$ ,  $\omega_1$ ,  $\omega_3$  and  $\omega_4$ . Similarly to the detailed-balance section these are subject to two constraints. The first one arises from the Friedman equation at  $z = 0$ , which leads to

$$\Omega_{m0} + \Omega_{r0} + \Omega_{K0} + \omega_1 + \omega_3 + \omega_4 = 1. \quad (36)$$

This constraint eliminates the parameter  $w_1$ .

The second constraint arises from BBN considerations. The term involving  $\omega_3$  represents the usual dark-radiation component. In addition, the  $\omega_4$ -term represents a kination-like component (a quintessence field dominated by kinetic energy [109, 110]). If  $\Delta N_\nu$  represents the BBN upper limit on the total energy density of the universe beyond standard model constituents, then as we show in the Appendix we acquire the following constraint at the time of BBN ( $z = z_{\text{BBN}}$ ) [105, 106, 107, 108]:

$$\omega_3 + \omega_4 (1 + z_{\text{BBN}})^2 = 0.135 \Delta N_\nu \Omega_{r0}. \quad (37)$$

It is clear that BBN imposes an extremely strong constraint on  $\omega_4$ , since its largest possible value (corresponding to  $\omega_3 = 0$ ) is  $\sim 10^{-24}$ .

We use relation (37) to eliminate  $\omega_4$  in favor of  $\omega_3$  and  $\Delta N_\nu$ , and treat  $\omega_3$  and  $\Omega_{K0}$  as our free parameters. Since  $\omega_4$  is non-negative, relation (37) determines also the upper bound of  $\omega_3$ . For the remaining parameters,  $\Omega_{m0}$  and  $H_0$  (unless otherwise stated) we assume priors corresponding to their 5-year WMAP best-fit values (given in Table 1 of [87]).

We now proceed to constrain the free parameters  $\Omega_{K0}$  and  $\omega_3$  through observations. Using the combined SNIa+CMB+BAO data, we construct likelihood contours for these two parameters. The details and the techniques of the construction are presented in the Appendix. Furthermore, since the BBN limits on  $\Delta N_\nu$  vary depending on assumptions, in addition to our canonical choice

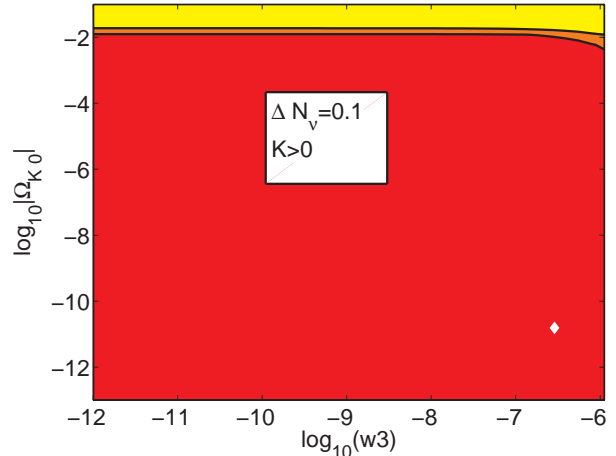


FIG. 3: (Color Online) Contour plots of  $\log_{10}(w_3)$  vs  $\log_{10}|\Omega_{K0}|$  for  $K > 0$  and  $\Delta N_\nu = 0.1$ , using SNIa, BAO and CMB data. The yellow (light) region is excluded at the  $2\sigma$  level, and the orange (darker) region is excluded at the  $1\sigma$  level. The red (darkest) region is not excluded at either confidence level. The white diamond marks the best-fit point.

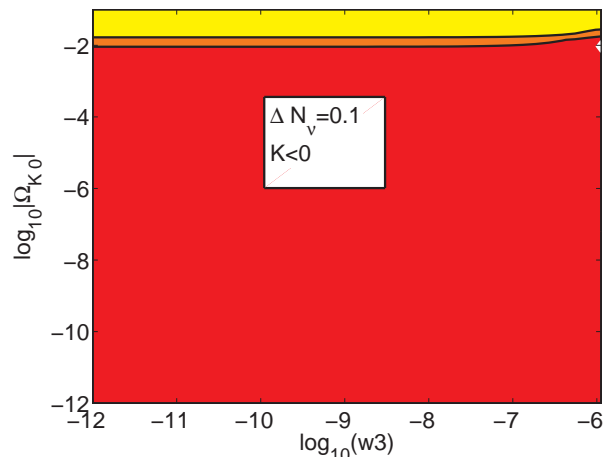


FIG. 4: (Color Online) Contour plots of  $\log_{10}(w_3)$  vs  $\log_{10}|\Omega_{K0}|$  for  $K < 0$  and  $\Delta N_\nu = 0.1$ , using SNIa, BAO and CMB data. The yellow (light) region is excluded at the  $2\sigma$  level, and the orange (darker) region is excluded at the  $1\sigma$  level. The red (darkest) region is not excluded at either confidence level. The white diamond marks the best-fit point (near the top right corner in this case).

$\sigma_0/(8\pi G)$	$\Delta N_\nu$	$\Omega_{K0}$	$(8\pi G/H_0^2) \sigma_1$	$\sigma_2$	$(8\pi G H_0^2) \sigma_3$	$\sigma_4/(8\pi G)$
1/3	0.1	(0, 0.01)	(4.29, 4.33)	-6	(0, 0.03)	$(-9.08 \times 10^{-22}, 0)$
1/3	0.1	(-0.01, 0)	(4.40, 4.45)	-6	(0, 0.81)	$(0, 5.66 \times 10^{-22})$
1/3	2.0	(0, 0.04)	(4.13, 4.45)	-6	(0, 0.01)	$(-1.77 \times 10^{-20}, -2.62 \times 10^{-21})$
1/3	2.0	(-0.01, 0)	(4.40, 4.45)	-6	(0, 0.23)	$(-2.61 \times 10^{-20}, -1.16 \times 10^{-20})$

TABLE II:  $1\sigma$  limits on the parameter values for the beyond-detailed-balance scenario, for positive and negative curvature, and for two values of the effective neutrino species parameter  $\Delta N_\nu$  (see text).

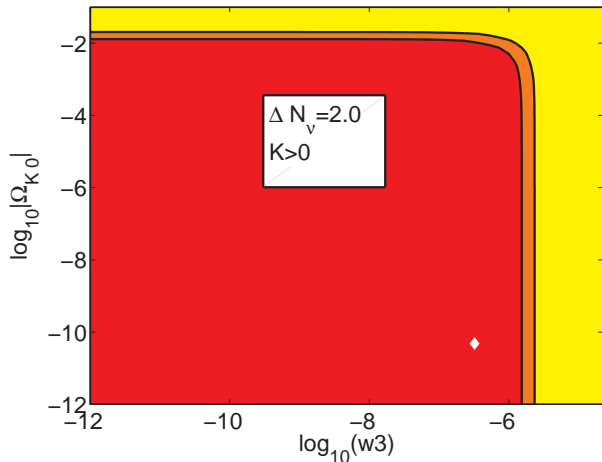


FIG. 5: (Color Online) Contour plots of  $\log_{10}(w_3)$  vs  $\log_{10}|\Omega_{K0}|$  for  $K > 0$  and  $\Delta N_\nu = 2.0$ , using SNIa, BAO and CMB data. The yellow (light) region is excluded at the  $2\sigma$  level, and the orange (darker) region is excluded at the  $1\sigma$  level. The red (darkest) region is not excluded at either confidence level. The white diamond marks the best-fit point.

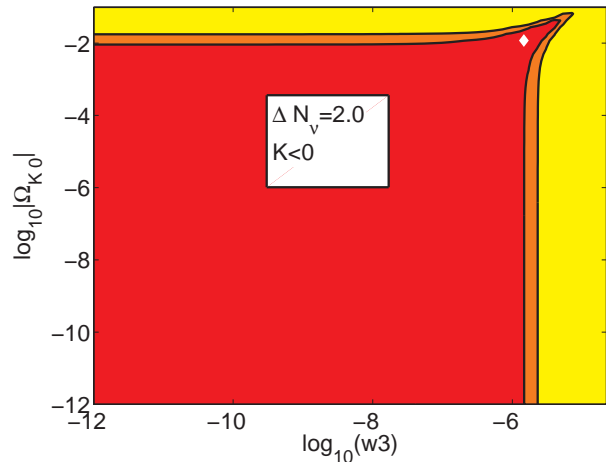


FIG. 6: (Color Online) Contour plots of  $\log_{10}(w_3)$  vs  $\log_{10}|\Omega_{K0}|$  for  $K < 0$  and  $\Delta N_\nu = 2.0$ , using SNIa, BAO and CMB data. The yellow (light) region is excluded at the  $2\sigma$  level, and the orange (darker) region is excluded at the  $1\sigma$  level. The red (darkest) region is not excluded at either confidence level. The white diamond marks the best-fit point.

of upper limit  $\Delta N_\nu = 2.0$ , we have also considered the more restrictive limit of  $\Delta N_\nu = 0.1$ .

Figures 3 and 4 depict the  $1\sigma$  and  $2\sigma$   $\omega_3 - |\Omega_{K0}|$  contours, for  $\Delta N_\nu = 0.1$ , for positive and negative curvature respectively. Figures 5 and 6 are the corresponding plots using  $\Delta N_\nu = 2$ . In each case,  $\omega_3$  extends over its entire allowed range, namely  $0 \leq \omega_3 \leq 0.135\Delta N_\nu\Omega_{r0}$ .

As we observe, the Hořava-Lifshitz cosmological scenario beyond the detailed balance condition is not ruled out by observations. However, they impose strong constraints on  $\omega_3$  (for the case of  $\Delta N_\nu = 2.0$  the constraints on  $\omega_3$  for both the positive and negative curvature cases are stronger than the upper bound from BBN), and extremely tight constraints on  $\omega_4$ . Additionally, the constraints on the curvature are of the order of a percent. Note that the contours expand as  $\Delta N_\nu$  is reduced. This is expected since the smaller the amount of exotic components (dark-radiation and kination-like ones), the closer the model is to  $\Lambda$ CDM.

The approximate  $1\sigma$  limits on the model parameters  $\sigma_i$  are presented in Table II. The lower limit on  $\sigma_3$  is zero. From (36) and (37) it is clear that  $\sigma_1$  and  $\sigma_4$  at-

tain their maximum values when  $\sigma_3$  is at its minimum, and vice versa. Similarly to the previous subsection, one can either use the usual ansatz  $8\pi G = H_0 = 1$ , or insert physical units using  $H_0 = 1.503 \times 10^{-42} \text{ GeV}$  and  $8\pi G = 1.681 \times 10^{-37} \text{ GeV}^{-2}$ . In the later case, one obtains that  $\sigma_1$  is tightly constrained to be at the level of the cosmological constant ( $10^{-12} \text{ eV}^4$ ), as expected. Additionally, the data impose extremely stringent constraints on  $\sigma_4$ , which was also expected. However, even for such small values, the phenomenological implications of the kination-like  $\sigma_4$ -component are very interesting. As discussed in detail in [111, 112], it could dominate the universe prior to BBN and it could significantly affect the freeze-out, and hence the relic abundances of neutralino dark matter, by a few orders of magnitude. For dark matter that decays into leptons (see e.g. [113]) this could be relevant to recent observations of high energy positrons and electrons by the PAMELA [114, 115] and ATIC [116] experiments.

## IV. CONCLUSIONS

In this work we constrained Hořava-Lifshitz cosmology using observational data. In particular, we considered scenarios where the gravitational sector is forced to satisfy the detailed-balance condition, and also those where this condition is relaxed. Additionally, we have included the matter and radiation sectors following the usual effective fluid approach. These constructions, which cover the range of Hořava-Lifshitz cosmology, were confronted with data from BBN, SNIa, CMB and BAO observations.

Our first result is that the detailed-balance formulation of Hořava-Lifshitz gravity cannot fulfill observational requirements, without the analytic-continuation transformation. Under the analytic continuation we found that Hořava-Lifshitz cosmology can be compatible with observations, and we presented the corresponding contour-plots on the model parameters. These likelihood-contours impose tight constraints on the model parameters, and the corresponding  $1\sigma$ -bounds are presented in Table I. However, we mention that although analytic continuation is necessary for a realistic cosmology, it can fatally affect the gravitational theory itself, spoiling its initial stability and well-behaving nature. Therefore, the detailed-balance version of Hořava-Lifshitz cosmology seems rather unlikely to be a robust description of nature.

The version of Hořava-Lifshitz cosmology in which the detailed-balance condition has been abandoned, is also compatible with observations. We constructed the likelihood-contours for the two involved free parameters, namely the curvature and the dark-radiation coefficients. As we showed, observations lead to strong bounds in these parameters, and the corresponding  $1\sigma$ -allowed ranges are presented in Table II. This feature was expected, since the data refer to redshifts in which the novel terms of Hořava-Lifshitz cosmology are downgraded. However, these terms can have significant cosmological implications prior to nucleosynthesis, which could be probed by recent observations of high energy positrons and electrons by the PAMELA [114, 115] and ATIC [116] experiments.

Although the present analysis indicates that Hořava-Lifshitz cosmology can be compatible with observations, it does not enlighten the discussion about possible conceptual problems and instabilities of Hořava-Lifshitz gravity, nor it can interfere with the questions concerning the validity of its theoretical background, which is the subject of interest of other studies. In particular, without a solid theoretical basis, it is not clear whether Hořava-Lifshitz gravity is able to pass the basic parametrized post newtonian (PPN) tests that any physically interesting gravitational theory should [117, 118, 119, 120]. The present work just faces the problem from the phenomenological point of view, and thus its results can be taken into account only if Hořava-Lifshitz gravity passes successfully the aforementioned theoretical tests.

## Acknowledgments

The authors would like to thank Bob Scherrer for useful discussions.

## APPENDIX: OBSERVATIONAL DATA AND CONSTRAINTS

In this appendix, we briefly review the main sources of observational constraints used in this work, namely, Big Bang Nucleosynthesis (BBN), Baryon Acoustic Oscillations (BAO) and the Cosmic Microwave Background (CMB).

### *a. Big Bang Nucleosynthesis constraints*

Big Bang Nucleosynthesis (BBN) provides a highly sensitive tool for probing physics beyond the standard model (for reviews see e.g. [105, 106, 107, 108]). Abundances of light elements predicted by BBN, particularly the  ${}^4\text{He}$  one, are sensitive to the expansion rate of the universe (or equivalently to its total energy density) at the time of BBN. Additionally, the abundances depend also on the baryon to photon ratio, though this ratio can be independently determined from the CMB by WMAP data [87]. BBN therefore imposes constraints on the densities of possible extra exotic radiation constituents (beyond the standard model photons and three flavors of neutrinos).

The constraints on the energy density of these exotic constituents are usually expressed in terms of the effective neutrino species  $\Delta N_\nu$ . Assuming that neutrinos are fully decoupled from photons and do not gain energy from  $e^\pm$  annihilation, they are colder than photons by a factor of  $T_\nu/T_\gamma = (4/11)^{1/3}$  (see e.g. [107]). Using also that the neutrino energy is related to the photon one by a factor of  $7/8$ , the total energy density of relativistic species - photons and  $(3 + \Delta N_\nu)$  species of neutrinos - reads

$$\rho_T = \rho_\gamma + (3 + \Delta N_\nu) \left(\frac{7}{8}\right) \left(\frac{4}{11}\right)^{4/3} \rho_\gamma. \quad (\text{A.1})$$

In terms of the total standard-model relativistic density (photons and three species of neutrinos)  $\rho_{\gamma\nu}$ , the above can be written as

$$\rho_T = (1 + 0.135\Delta N_\nu) \rho_{\gamma\nu}. \quad (\text{A.2})$$

In the present work we use the upper limits on  $\Delta N_\nu$  provided in [107]:  $-1.7 \leq \Delta N_\nu \leq 2.0$ , although more restrictive bounds have also been proposed (see e.g. [121, 122]). We mention that the above limits do not apply to models in which the dark radiation or other exotic components are injected later than BBN (see [123] for an example of such a model), however they are obviously applicable to Hořava-Lifshitz cosmology, in which dark radiation is always present, arising from the

gravitational theory itself.

*b. Type Ia Supernovae constraints*

In order to incorporate supernova constraints we use the Union08 compilation of SnIa data [124]. This is a heterogeneous data-set, consisting of data from the Supernova Legacy Survey, the Essence survey, the recently extended data-set of distant supernovae observed by the Hubble Space Telescope, as well as older data-sets.

The  $\chi^2$  from SNIa is calculated as:

$$\chi_{SN}^2 = \frac{\sum_{i=1}^N [\mu_{\text{obs}}(z_i) - \mu_{\text{th}}(z_i)]^2}{\sigma_{\mu,i}^2}, \quad (\text{A.3})$$

where  $N = 307$  is the number of SNIa data points.  $\mu_{\text{obs}}$  is the observed distance modulus, defined as the difference between the apparent and absolute magnitude of the supernova. The  $\sigma_{\mu,i}$  are the errors in the observed distance moduli, arising from a variety of sources, and assumed to be gaussian and uncorrelated. The theoretical distance modulus  $\mu_{\text{th}}$  depends on the model parameters  $a_i$  via the dimensionless luminosity distance  $D_L(z; a_i)$ :

$$D_L(z; a_i) \equiv (1+z) \int_0^z dz' \frac{H_0}{H(z'; a_i)}, \quad (\text{A.4})$$

as follows:

$$\mu_{\text{th}}(z) = 42.38 - 5 \log_{10} h + 5 \log_{10} [D_L(z; a_i)]. \quad (\text{A.5})$$

The marginalization over the present value of the Hubble parameter is performed following the techniques described in [125], and we construct  $\chi^2$  likelihood contours for the various model parameters.

*c. CMB constraints*

We use the CMB data to impose constraints on the parameter space, following the recipe described in [87]. The ‘‘CMB shift parameters’’ [99, 126] are defined as:

$$R \equiv \sqrt{\Omega_{m0}} H_0 r(z_*), \quad l_a \equiv \pi r(z_*) / r_s(z_*). \quad (\text{A.6})$$

$R$  can be physically interpreted as a scaled distance to recombination, and  $l_a$  can be interpreted as the angular scale of the sound horizon at recombination.  $r(z)$  is the comoving distance to redshift  $z$  defined as

$$r(z) \equiv \int_0^z \frac{1}{H(z)} dz, \quad (\text{A.7})$$

while  $r_s(z_*)$  is the comoving sound horizon at decoupling (redshift  $z_*$ ), given by

$$r_s(z_*) = \int_{z_*}^{\infty} \frac{1}{H(z) \sqrt{3(1 + R_b/(1+z))}} dz. \quad (\text{A.8})$$

The quantity  $R_b$  is the ratio of the energy density of photons to baryons, and its value can be calculated as  $R_b =$

$31500 \Omega_{b0} h^2 (T_{CMB}/2.7K)^{-4}$ , ( $\Omega_{b0}$  being the present day density parameter for baryons) using  $T_{CMB} = 2.725$  [87]. The redshift at decoupling  $z_*$  ( $\Omega_{b0}, \Omega_{m0}, h$ ) can be calculated from the following fitting formula [127]:

$$z_* = 1048 \left[ 1 + 0.00124 (\Omega_{b0} h^2)^{-0.738} \right] \left[ 1 + g_1 (\Omega_{m0} h^2)^{g_2} \right], \quad (\text{A.9})$$

with  $g_1$  and  $g_2$  given by:

$$g_1 = \frac{0.0783 (\Omega_{b0} h^2)^{-0.238}}{1 + 39.5 (\Omega_{b0} h^2)^{0.763}}$$

$$g_2 = \frac{0.560}{1 + 21.1 (\Omega_{b0} h^2)^{1.81}}.$$

Finally, the  $\chi^2$  contribution of the CMB reads

$$\chi_{CMB}^2 = \mathbf{V}_{CMB}^T \mathbf{C}_{\text{inv}} \mathbf{V}_{CMB}. \quad (\text{A.10})$$

Here  $\mathbf{V}_{CMB} \equiv \mathbf{P} - \mathbf{P}_{\text{data}}$ , where  $\mathbf{P}$  is the vector ( $l_a, R, z_*$ ) and the vector  $\mathbf{P}_{\text{data}}$  is formed from the WMAP 5-year maximum likelihood values of these quantities [87]. The inverse covariance matrix  $\mathbf{C}_{\text{inv}}$  is also provided in [87].

*d. Baryon Acoustic Oscillation constraints*

In this case the measured quantity is the ratio  $d_z = r_s(z_d)/D_V(z)$ , where  $D_V(z)$  is the so called ‘‘volume distance’’, defined in terms of the angular diameter distance  $D_A \equiv r(z)/(1+z)$  as

$$D_v(z) \equiv \left[ \frac{(1+z)^2 D_A^2(z) z}{H(z)} \right]^{1/3}, \quad (\text{A.11})$$

and  $z_d$  is the redshift of the baryon drag epoch, which can be calculated from the fitting formula [128]:

$$z_d = \frac{1291 (\Omega_{m0} h^2)^{0.251}}{1 + (\Omega_{M0} h^2)^{0.828}} \left[ 1 + b_1 (\Omega_{b0} h^2)^{b_2} \right], \quad (\text{A.12})$$

where  $b_1$  and  $b_2$  are given by

$$b_1 = 0.313 (\Omega_{m0} h^2)^{-0.419} \left[ 1 + 0.607 (\Omega_{m0} h^2)^{0.674} \right]$$

$$b_2 = 0.238 (\Omega_{m0} h^2)^{0.223}.$$

We use the two measurements of  $d_z$  at redshifts  $z = 0.2$  and  $z = 0.35$  [129]. We calculate the  $\chi^2$  contribution of the BAO measurements as:

$$\chi_{BAO}^2 = \mathbf{V}_{BAO}^T \mathbf{C}_{\text{inv}} \mathbf{V}_{BAO}. \quad (\text{A.13})$$

Here the vector  $\mathbf{V}_{BAO} \equiv \mathbf{P} - \mathbf{P}_{\text{data}}$ , with  $\mathbf{P} \equiv (d_{0.2}, d_{0.35})$ , and  $\mathbf{P}_{\text{data}} \equiv (0.1905, 0.1097)$ , the two measured BAO data points [129]. The inverse covariance matrix is provided in [129].

- 
- [1] P. Horava, arXiv:0811.2217 [hep-th].
- [2] P. Horava, *JHEP* **0903**, 020 (2009) [arXiv:0812.4287 [hep-th]].
- [3] P. Horava, *Phys. Rev. D* **79**, 084008 (2009) [arXiv:0901.3775 [hep-th]].
- [4] P. Hořava, arXiv:0902.3657 [hep-th].
- [5] G. E. Volovik, arXiv:0904.4113 [gr-qc].
- [6] R. G. Cai, Y. Liu and Y. W. Sun, arXiv:0904.4104 [hep-th].
- [7] R. G. Cai, B. Hu and H. B. Zhang, arXiv:0905.0255 [hep-th].
- [8] D. Orlando and S. Reffert, arXiv:0905.0301 [hep-th].
- [9] T. Nishioka, arXiv:0905.0473 [hep-th].
- [10] R. A. Konoplya, arXiv:0905.1523 [hep-th].
- [11] C. Charmousis, G. Niz, A. Padilla and P. M. Saffin, arXiv:0905.2579 [hep-th].
- [12] T. P. Sotiriou, M. Visser and S. Weinfurtner, *Phys. Rev. Lett.* **102**, 251601 (2009) [arXiv:0904.4464 [hep-th]].
- [13] T. P. Sotiriou, M. Visser and S. Weinfurtner, *JHEP* **0910**, 033 (2009) [arXiv:0905.2798 [hep-th]].
- [14] C. Germani, A. Kehagias and K. Sfetsos, *JHEP* **0909**, 060 (2009) [arXiv:0906.1201 [hep-th]].
- [15] C. Bogdanos and E. N. Saridakis, arXiv:0907.1636 [hep-th].
- [16] J. Kluson, arXiv:0907.3566 [hep-th].
- [17] N. Afshordi, arXiv:0907.5201 [hep-th].
- [18] Y. S. Myung, arXiv:0907.5256 [hep-th].
- [19] J. Alexandre, K. Farakos, P. Pasipoularides and A. Tsapalis, arXiv:0909.3719 [hep-th].
- [20] D. Blas, O. Pujolas and S. Sibiryakov, arXiv:0909.3525 [hep-th].
- [21] D. Capasso and A. P. Polychronakos, arXiv:0909.5405 [hep-th].
- [22] B. Chen, S. Pi and J. Z. Tang, arXiv:0910.0338 [hep-th].
- [23] J. Kluson, arXiv:0910.5852 [hep-th].
- [24] M. Li and Y. Pang, arXiv:0905.2751 [hep-th].
- [25] M. Visser, arXiv:0902.0590 [hep-th].
- [26] J. Chen and Y. Wang, arXiv:0905.2786 [gr-qc].
- [27] B. Chen and Q. G. Huang, arXiv:0904.4565 [hep-th].
- [28] F. W. Shu and Y. S. Wu, arXiv:0906.1645 [hep-th].
- [29] G. Calcagni, arXiv:0904.0829 [hep-th].
- [30] E. Kiritsis and G. Kofinas, arXiv:0904.1334 [hep-th].
- [31] H. Lu, J. Mei and C. N. Pope, arXiv:0904.1595 [hep-th].
- [32] H. Nastase, arXiv:0904.3604 [hep-th].
- [33] E. O. Colgain and H. Yavartanoo, arXiv:0904.4357 [hep-th].
- [34] A. Ghodsi, arXiv:0905.0836 [hep-th].
- [35] M. Minamitsuji, arXiv:0905.3892 [astro-ph.CO].
- [36] A. Ghodsi and E. Hatefi, arXiv:0906.1237 [hep-th].
- [37] P. Wu and H. W. Yu, arXiv:0909.2821 [gr-qc].
- [38] I. Cho and G. Kang, arXiv:0909.3065 [hep-th].
- [39] C. G. Boehmer and F. S. N. Lobo, arXiv:0909.3986 [gr-qc].
- [40] D. Momeni, arXiv:0910.0594 [gr-qc].
- [41] S. Carloni, E. Elizalde and P. J. Silva, arXiv:0909.2219 [hep-th].
- [42] G. Leon and E. N. Saridakis, *JCAP* **0911**, 006 (2009) [arXiv:0909.3571 [hep-th]].
- [43] S. Mukohyama, K. Nakayama, F. Takahashi and S. Yokoyama, arXiv:0905.0055 [hep-th].
- [44] T. Takahashi and J. Soda, arXiv:0904.0554 [hep-th].
- [45] S. Koh, arXiv:0907.0850 [hep-th].
- [46] M. i. Park, arXiv:0910.1917 [hep-th].
- [47] M. i. Park, arXiv:0910.5117 [hep-th].
- [48] Y. S. Myung, arXiv:0911.0724 [hep-th].
- [49] S. Mukohyama, arXiv:0904.2190 [hep-th].
- [50] Y. S. Piao, arXiv:0904.4117 [hep-th].
- [51] X. Gao, arXiv:0904.4187 [hep-th].
- [52] B. Chen, S. Pi and J. Z. Tang, arXiv:0905.2300 [hep-th].
- [53] X. Gao, Y. Wang, R. Brandenberger and A. Riotto, arXiv:0905.3821 [hep-th].
- [54] Y. F. Cai and X. Zhang, *Phys. Rev. D* **80**, 043520 (2009) [arXiv:0906.3341 [astro-ph.CO]].
- [55] A. Wang and R. Maartens, arXiv:0907.1748 [hep-th].
- [56] T. Kobayashi, Y. Urakawa and M. Yamaguchi, arXiv:0908.1005 [astro-ph.CO].
- [57] A. Wang, D. Wands and R. Maartens, arXiv:0909.5167 [hep-th].
- [58] R. Brandenberger, arXiv:0904.2835 [hep-th].
- [59] R. H. Brandenberger, arXiv:0905.1514 [hep-th].
- [60] Y. F. Cai and E. N. Saridakis, *JCAP* **0910**, 020 (2009) [arXiv:0906.1789 [hep-th]].
- [61] T. Suyama, arXiv:0909.4833 [hep-th].
- [62] U. H. Danielsson and L. Thorlacius, *JHEP* **0903**, 070 (2009) [arXiv:0812.5088 [hep-th]].
- [63] R. G. Cai, L. M. Cao and N. Ohta, arXiv:0904.3670 [hep-th].
- [64] Y. S. Myung and Y. W. Kim, arXiv:0905.0179 [hep-th].
- [65] A. Kehagias and K. Sfetsos, *Phys. Lett. B* **678**, 123 (2009) [arXiv:0905.0477 [hep-th]].
- [66] R. B. Mann, arXiv:0905.1136 [hep-th].
- [67] G. Bertoldi, B. A. Burrington and A. Peet, arXiv:0905.3183 [hep-th].
- [68] M. i. Park, *JHEP* **0909**, 123 (2009) [arXiv:0905.4480 [hep-th]].
- [69] A. Castillo and A. Larranaga, arXiv:0906.4380 [gr-qc].
- [70] M. Botta-Cantcheff, N. Grandi and M. Sturla, arXiv:0906.0582 [hep-th].
- [71] H. W. Lee, Y. W. Kim and Y. S. Myung, arXiv:0907.3568 [hep-th].
- [72] N. Varghese and V. C. Kuriakose, arXiv:0909.4944 [gr-qc].
- [73] E. Kiritsis and G. Kofinas, arXiv:0910.5487 [hep-th].
- [74] E. N. Saridakis, arXiv:0905.3532 [hep-th].
- [75] M. i. Park, arXiv:0906.4275 [hep-th].
- [76] C. Appignani, R. Casadio and S. Shankaranarayanan, arXiv:0907.3121 [hep-th].
- [77] M. R. Setare, arXiv:0909.0456 [hep-th].
- [78] S. S. Kim, T. Kim and Y. Kim, arXiv:0907.3093 [hep-th].
- [79] T. Harko, Z. Kovacs and F. S. N. Lobo, arXiv:0908.2874 [gr-qc].
- [80] L. Iorio and M. L. Ruggiero, arXiv:0909.2562 [gr-qc].
- [81] L. Iorio and M. L. Ruggiero, arXiv:0909.5355 [gr-qc].
- [82] A. Wang and Y. Wu, arXiv:0905.4117 [hep-th].
- [83] R. G. Cai, L. M. Cao and N. Ohta, arXiv:0905.0751 [hep-th].
- [84] R. G. Cai and N. Ohta, arXiv:0910.2307 [hep-th].
- [85] K. Koyama and F. Arroja, arXiv:0910.1998 [hep-th].
- [86] A. Papazoglou and T. P. Sotiriou, arXiv:0911.1299 [hep-th].
- [87] E. Komatsu *et al.* [WMAP Collaboration], *Astrophys.*

- J. Suppl. **180**, 330 (2009) [arXiv:0803.0547 [astro-ph]].
- [88] A. R. Liddle and R. J. Scherrer, Phys. Rev. D **59**, 023509 (1999) [arXiv:astro-ph/9809272].
- [89] R. Dave, R. R. Caldwell and P. J. Steinhardt, Phys. Rev. D **66**, 023516 (2002) [arXiv:astro-ph/0206372].
- [90] D. C. Dai, S. Dutta and D. Stojkovic, Phys. Rev. D **80**, 063522 (2009) [arXiv:0909.0024 [astro-ph.CO]].
- [91] T. Chiba, S. Dutta and R. J. Scherrer, Phys. Rev. D **80**, 043517 (2009) [arXiv:0906.0628 [astro-ph.CO]].
- [92] S. Dutta, E. N. Saridakis and R. J. Scherrer, Phys. Rev. D **79**, 103005 (2009) [arXiv:0903.3412 [astro-ph.CO]].
- [93] S. Dutta and R. J. Scherrer, Phys. Lett. B **676**, 12 (2009) [arXiv:0902.1004 [astro-ph.CO]].
- [94] S. Dutta and R. J. Scherrer, Phys. Rev. D **78**, 123525 (2008) [arXiv:0809.4441 [astro-ph]].
- [95] S. Dutta and R. J. Scherrer, Phys. Rev. D **78**, 083512 (2008) [arXiv:0805.0763 [astro-ph]].
- [96] J. L. Crooks, J. O. Dunn, P. H. Frampton, H. R. Norton and T. Takahashi, Astropart. Phys. **20**, 361 (2003) [arXiv:astro-ph/0305495].
- [97] K. Ichikawa and T. Takahashi, Phys. Rev. D **73**, 083526 (2006) [arXiv:astro-ph/0511821].
- [98] G. Barenboim, E. Fernandez-Martinez, O. Mena and L. Verde, arXiv:0910.0252 [astro-ph.CO].
- [99] Y. Wang and P. Mukherjee, Phys. Rev. D **76**, 103533 (2007) [arXiv:astro-ph/0703780].
- [100] E. L. Wright, Astrophys. J. **664**, 633 (2007) [arXiv:astro-ph/0701584].
- [101] K. Ichikawa, M. Kawasaki, T. Sekiguchi and T. Takahashi, JCAP **0612**, 005 (2006) [arXiv:astro-ph/0605481].
- [102] K. Ichikawa and T. Takahashi, JCAP **0702**, 001 (2007) [arXiv:astro-ph/0612739].
- [103] C. Clarkson, M. Cortes and B. A. Bassett, JCAP **0708**, 011 (2007) [arXiv:astro-ph/0702670].
- [104] J. M. Virey, D. Talon-Esmieu, A. Ealet, P. Taxil and A. Tilquin, JCAP **0812**, 008 (2008) [arXiv:0802.4407 [astro-ph]].
- [105] K. Hagiwara *et al.* [Particle Data Group], Phys. Rev. D **66**, 010001 (2002).
- [106] K. A. Olive, G. Steigman and T. P. Walker, Phys. Rept. **333**, 389 (2000) [arXiv:astro-ph/9905320].
- [107] G. Steigman, Int. J. Mod. Phys. E **15**, 1 (2006) [arXiv:astro-ph/0511534].
- [108] R. A. Malaney and G. J. Mathews, Phys. Rept. **229**, 145 (1993).
- [109] M. Joyce, Phys. Rev. D **55**, 1875 (1997) [arXiv:hep-ph/9606223].
- [110] M. Joyce and T. Prokopec, Phys. Rev. D **57**, 6022 (1998) [arXiv:hep-ph/9709320].
- [111] P. Salati, Phys. Lett. B **571**, 121 (2003) [arXiv:astro-ph/0207396].
- [112] C. Pallis, arXiv:0909.3026 [hep-ph].
- [113] Q. H. Cao, E. Ma and G. Shaughnessy, Phys. Lett. B **673**, 152 (2009) [arXiv:0901.1334 [hep-ph]].
- [114] O. Adriani *et al.* [PAMELA Collaboration], Nature **458**, 607 (2009) [arXiv:0810.4995 [astro-ph]].
- [115] O. Adriani *et al.*, Phys. Rev. Lett. **102**, 051101 (2009) [arXiv:0810.4994 [astro-ph]].
- [116] J. Chang *et al.*, Nature **456**, 362 (2008).
- [117] L. I. Schiff, Proc. Nat. Acad. Sci. **46**, 871 (1960).
- [118] K. Nordtvedt, Phys. Rev. **169**, 1017 (1968).
- [119] C. M. Will, Astrophys. J. **163**, 611 (1971).
- [120] C. M. Will, *Theory and experiment in gravitational physics*, Cambridge University Press, Cambridge, UK (1993).
- [121] A. R. Zentner and T. P. Walker, Phys. Rev. D **65**, 063506 (2002) [arXiv:astro-ph/0110533].
- [122] R. Bean, S. H. Hansen and A. Melchiorri, Nucl. Phys. Proc. Suppl. **110**, 167 (2002) [arXiv:astro-ph/0201127].
- [123] S. Dutta, S. D. H. Hsu, D. Reeb and R. J. Scherrer, Phys. Rev. D **79**, 103504 (2009) [arXiv:0902.4699 [astro-ph.CO]].
- [124] M. Kowalski *et al.*, Astrophys. J. **686**, 749 (2008) [arXiv:0804.4142 [astro-ph]].
- [125] R. Lazkoz, S. Nesseris and L. Perivolaropoulos, JCAP **0807**, 012 (2008) [arXiv:0712.1232 [astro-ph]].
- [126] Y. Wang and P. Mukherjee, Astrophys. J. **650**, 1 (2006) [arXiv:astro-ph/0604051].
- [127] W. Hu and N. Sugiyama, Astrophys. J. **471**, 542 (1996) [arXiv:astro-ph/9510117].
- [128] D. J. Eisenstein and W. Hu, Astrophys. J. **496**, 605 (1998) [arXiv:astro-ph/9709112].
- [129] W. J. Percival *et al.*, arXiv:0907.1660 [astro-ph.CO].